Zagazig University Medical Journal
www.zumj.journals.ekb.eg
https://doi.org/10.21608/zumj.2024.280708.3301 Volume 30, Issue 1.4, June 2024, Supplement Issue
Manuscript ID ZUMJ-2403-3301 (R2)
DOI 10.21608/ZUMJ.2024.280708.3301
ORIGINAL ARTICLE

Effect of Mesenchymal Stem Cells-Conditioned Medium versus Silymarin on Experimentally Induced Fatty Liver in Adult Male Albino Rats: A Histological and Immunohistochemical Study

Ebtehal Z. Hassan[1], Rania A. Zidan[1], Susanna N. Mesiha[1*], Samaa M. El-Mahroky[1]
[1]Department of Medical Histology and Cell Biology, Faculty of Medicine, Zagazig University, Egypt.

Corresponding author:
Susanna Nabil Kamal

Email:
sosananabil22@gmail.com

Submit Date 2024-04-03
Revise Date 2024-05-15
Accept Date 2024-05-18

ABSTRACT

Background: Fatty liver is the most prevalent chronic liver disease. The progressive form of fatty liver disease is non-alcoholic steatohepatitis (NASH), which can lead to liver fibrosis and cirrhosis. Silymarin is a traditional liver treatment while Mesenchymal stem cells conditioned medium (MSCs-CM) is a new hope for treatment of chronic liver diseases. Our aim is to evaluate the effect of MSCs-CM versus Silymarin on experimentally induced fatty liver in adult male albino rats.

Methods: Fifty-four adult male albino rats were divided into four groups: I (control group 27 rats) divided into 3 subgroups: (Subgroup Ia, Ib and Ic), II (fatty liver group), III (fatty liver -Silymarin) and IV (fatty liver -MSC-CM). Blood samples were collected for lipid profile. Liver tissue was prepared for H&E staining, Mallory's trichrome staining, osmic acid staining, immunohistochemically staining for alpha smooth muscle actin (α-SMA) and caspase 3 and electron microscope examination. Statistical and morphometrical studies were performed.

Results: Regarding lipid profile, α-SMA and caspase-3 the highest mean values were observed in group II while the least in group IV. H&E-stained sections of group II showed degenerated hepatocytes with vacuolated cytoplasm and darkly stained nuclei. Ultra-structurally, group II revealed, rarified cytoplasm with swollen mitochondria and bundles of collagen while in group III showed some improvement, group IV most of hepatocytes appeared normal.

Conclusions: MSCs-CM has a more ameliorative effect than Silymarin on induced non-alcoholic fatty liver disease through its anti-apoptotic and anti-inflammatory effects.

Keywords: MSCs-CM, Silymarin, NASH, Fatty Liver; High lipid diet.

INTRODUCTION

Currently, non-alcoholic fatty liver disease (NAFLD) is the most prevalent chronic liver disease worldwide. The prevalence of obesity and type 2 diabetes mellitus is rising along with the incidence of NAFLD globally. NAFLD is anticipated to impact nearly one billion people worldwide and could be found in about 25% of people worldwide. Globally, non-obese persons with NAFLD have rates ranging from 10% to 30% in Western and Eastern nations **[1]**.

There are two subtypes of NAFLD. The progressive form of NAFLD is called non-alcoholic steatohepatitis (NASH), and it is more severe than the non-progressive form, which is called non-alcoholic fatty liver (NAFL). NASH can result in fibrosis and cirrhosis. NASH initial presentation is hepatic steatosis **[2, 3].**

Diet rich in fat and lipid in humans may cause hepatic steatosis. It was found that overweight women without diabetes who consumed a high fat, isocaloric diet for two weeks (56% of total energy

from fat) show a 35% rise in liver fat. A high-fat, high-energy diet for three days caused considerable increases in liver triglycerides (TG), non-esterified fatty acid (NEFA), and plasma TG in healthy men **[3]**.

In general, men are more likely than women to have NAFLD. The prevalence of NAFLD in males tends to rise in middle age and then decline beyond the age fifty. In women beyond the age of fifty, the frequency is lower, but it increases after menopause and peaks at the age of age sixty **[4].**

Insulin resistance (IR) and hyperinsulinemia are related to visceral obesity. Hepatic lipid accumulation can be used to diagnose IR in the absence of fat deposition and peripheral organ IR. Silymarin lowers IR by lowering visceral fat and by reducing hepatic gluconeogenesis by blocking the major enzymes of this metabolic pathway, phosphoenolpyruvate carboxykinase (PEPCK) and glucose 6 phosphatase (G6Pase) **[5].**

Silymarin has been widely used in treating gallbladder and liver diseases especially hepatitis, cirrhosis, and fatty liver disease **[6, 7].**

Conditioned medium was also found to improve insulin resistance in diabetic mice, improves mitochondrial activity, the antioxidant capacity of the entire liver and corrects the liver pathology **[8]**.

Conditioned medium also contains microRNA, membrane vesicles, nucleic acids, exosomes, and proteasomes. Most of the therapeutic effects offered by Mesenchymal stem cells (MSCs) have been linked to these MSC-secreted components within conditioned media, also referred to as the MSC "secretome." **[9].**

Aim of the work:

To evaluate the effect of MSCs-CM versus Silymarin on experimentally induced fatty liver in adult male albino rats.

METHODS

- **Animals:**

Fifty-four adult healthy male albino rats weighing between 180 and 200 grams. Rats were acquired from the Animal House at Zagazig University's Faculty of Medicine in Egypt. The Zagazig University IACUC Committee evaluated and approved the experiment's protocol; **ZU-IACUC/3/F/98/2023** was the protocol approval number.

Chemicals:

Silymarin was purchased as a powder from Sigma-Aldrich. It was administered orally by gavage after being dissolved in distilled water **[10].**

Mesenchymal stem cells conditioned medium (MSCs-CM): was obtained from Medical Biochemistry and Molecular Biology Department, Zagazig University.

- **Preparation of adipose derived mesenchymal stem cells conditioned media (AD-MSCs-CM):**

For collecting the conditioned media: 1×10^6 AD-MSCs at passage 3 were cultured in T75 tissue culture flask **[11].** MSCs in culture were characterized by rounded, spindle like or fusiform shape and their characteristic adhesiveness detected by inverted microscope **[12].** The next day, Garamycin (0.05 mg/mL) and 2.4 ml of Dulbecco's Modified Eagle Medium (DMEM) were added to cultures. Conditioned Media (supernatants) were collected after 24 or 48 hours and MSCs were analyzed and centrifuged at 2000 rpm for 10 min **[13].** After collecting the conditioned medium, cellular debris was eliminated by filtering them through a 0.2-µm filter. The prepared media were kept frozen at minus eighty °C (-80°C) for later use. **[11].**

- **Diets used in this study:**

- Standard rat chow diet consists of pellets that include 70% carbs, 4% fat, 20% protein, 3% fiber, 2% mineral salts and 1% vitamin (Meladco for Animal Food, El-Obour, Egypt).

- Preparation of high lipid diet formed of a mixture of coconut oil (NABTAH virgin coconut oil) and vanaspati (vegetable) ghee (El-Aseel vegetable ghee) (hydrogenated, solidified palm oil) in a ratio of 2:3. Components of high lipid diet were bought in the neighborhood market.

- **Experimental design:**

- Rats were divided into four groups:

Group I (control group): This group consists of 27 rats were equally divided into 3 sub-groups: Subgroup Ia (negative control): did not receive any treatment for 8 weeks, subgroup Ib (Silymarin treated group) supplied with Silymarin at a dose of (100 mg/kg) by means of oral gavage daily for **[14]** for the last 4 weeks (from week 5 to week 8) **[15]** and Subgroup Ic (Mesenchymal Stem Cells-Conditioned Medium (MSC-CM) group): fed a standard chow diet for 8 weeks and injected with 200µl (AD-MSCs-CM): via tail vein for each rat **[16]** twice per week on two successive days (24 hours apart) **[17]** for the last four weeks (from week 5 to week 8) **[18].**

Group II fatty liver group (FL group): This group includes nine rats which were given high lipid diet of (coconut oil and vanaspati ghee using a 2:3 ratio)

orally through gavage in a dose of 10 mL/kg body weight) **[19]** daily for eight weeks and at the same time, rats would be allowed free access to balanced diet ad libitum **[20]**.

Group III fatty liver group treated with Silymarin (FL- Silymarin): This group includes nine rats that were given high lipid diet by the same dose and duration as group II and concomitantly supplied with Silymarin at a dose of (100 mg/kg) by means of oral gavage daily **[14]** for the last 4 weeks (from week 5 to week 8) **[15].**

Group IV (fatty liver group treated with Mesenchymal Stem Cells-Conditioned Media) (FL-MSC-CM): This group includes nine rats that were given high lipid diet by the same dose and duration as group II and concomitantly injected with 200µl (AD-MSCs-CM): via tail vein for each rat **[16]** twice per week on two successive days (24 hours apart) **[17]** for the last four weeks (from week 5 to week 8) **[18].**

- **Biochemical study**

At the end of the experiment, after 12 h fasting blood was collected using capillary tubes from retro orbital veins and serum lipid profile, which includes TG, total cholesterol (TC), HDL (high density lipoprotein) and LDL (low density lipoprotein), were measured using Abcam ab65390 HDL and LDL, Cholesterol assay kit (colorimetric/flurometric) and TR 20 30 for triglycerides **[21]**.

- **Histological study**

All animals were sedated with an intraperitoneal injection of euthanasia (60 ml/kg of phenobarbitone) and subsequently slaughtered at the conclusion of the experiment **[22]** 6 days after the last dose of injection of conditioned media **[23].** Liver tissues were taken for examination under light and electron microscopes.

- **Light microscopic technique:**

Each animal's liver was thoroughly dissected, and the tissues were immediately submerged in 10% formol saline for 48 hours before being processed and embedded in paraffin to prepare 5 micrometer-thick paraffin sections and then stained with:

- **H&E** for histological analysis **[24].**
- **Mallory's trichrome** for demonstration of collagen fibers distribution in the liver. Paraffin sections were processed and stained by celestine blue hematoxylin alum method **[24].**
- **Osmium tetraoxide stain:** A tiny sample measuring 0.5× 0.5× 0.5 cubic centimeter in 10% neutral buffer formalin, then were transferred to 2% osmic acid for 3-5 days as post fixative, before being processed and embedded in paraffin to prepare sections of 3 micrometer in thickness with a conventional microtome **[25, 26].**
- **Immunohistochemical stain:**

Alpha-smooth muscle actin (α-SMA): hepatic stellate cells (HSCs) activation marker **[27].**

Caspase 3: marker for apoptosis **[28].**

Primary and secondary antibodies were applied to the 5µm-thick sections. The primary antibody for α-SMA is α-SMA antibody, which is a monoclonal antibody of the IgG immunoglobulin type expressed in mice. Sigma Biochemical (St. Louis, Missouri, USA) provided it. The main antibody against caspase 3 is an IgG-type rabbit monoclonal antibody obtained from Lab Vision Laboratories (CAT #: 14751) Using a counterstain of Mayer's hematoxylin, (3′-DHP) 3′-diaminobenzidine-hydrogen peroxide was used to visualize immunoreactivity. Digital cameras were utilized to take images and an Olympus microscope was used for examination. Photomicrographs were accompanied with scale bars **[29].**

- **Transmission electron microscope technique:**

Tissue specimens were cut into small pieces (1.0 mm^3) for electron microscopy investigations. They were then postfixed in 1% osmium tetroxide in 0.1 M cacodylate buffer at pH 7.4 and 4 °C for two hours after being prefixed in 2.5% glutaraldehyde for 24 hours. After dehydration, the specimens were immersed in increasing alcohol concentrations for 15 minutes—50%, 70%, 90%, and 95%, respectively—and then in 100% alcohol for another 15 minutes (two changes). Propylene oxide was added to the specimens for 30 minutes (two changes) at room temperature. This allowed the epoxy resin to easily infiltrate the tissues and rapidly replace the dehydrating agent. Subsequently, the samples were placed in a 1:1 resin and propylene oxide mixture. After shaking the vial to combine the ingredients, it was set on a specimen rotator for an hour. After that pure epoxy resin was used to replace the mixture, and the vials were left on the rotator for the entire night. In order to create resin blocks, the specimens were immersed in flat capsules in epoxy resin and polymerized for 24 hours at 60 C. Using a Leica ultra-cut, semithin (1µm) and ultrathin (70–90 nanometer) sections were cut. Toluidine blue (1%) was used to stain semithin sections which were examined under a light microscope. TEM was used

to examine and photograph the ultrathin sections. (JEOL TEM 2100, Jeol Ltd, Tokyo, Japan) in the Electron Microscope Unit, Faculty of Agriculture, El Mansoura University, Egypt, and by TEM (JEOL JEM100CX, Jeol Ltd, Tokyo, Japan) in the Electron Microscope Unit, Faculty of Science, Zagazig University, Egypt **[30].**

Statistical Analysis

(SPSS Inc., Chicago, Illinois, USA), the statistical programme for social sciences, version 21, was used to analyze the recorded data. The statistical information was presented as mean ± standard deviation (SD). To assess the differences between the mean values of the experimental groups, a one-way analysis of variance (ANOVA) was used. Tukey's multiple comparison test was used for the post hoc analysis of the ANOVA. The results were deemed statistically significant when the P value of 0.05 was deemed negligible **[31].**

RESULTS

General observational results (Table 1):

Throughout the duration of the experiment, none of the animals in the study groups died as a result of their treatments.

Since the liver index (liver weight/ body weight x 100) data from the control subgroups (Ia, Ib, and Ic) were almost the same, the findings of each were merged and presented as a single control group for statistical analysis. The liver index varied significantly among the four groups under study, with group 1 having the lowest level and group 2 having the highest level. Group 2 had a statistically significant rise when compared to group 1, whereas group 3 showed a statistically significant decrease when compared to group 2. With no statistically significant difference between it and group 1, group 4 had a high statistically lower liver index than groups 2 and 3.

Biochemical results (Figure 1s; Table 1):

Lipid profile:

A statistically significant difference was noticed in the different groups under study. The FL group demonstrated a substantial statistical rise in serum levels of LDL, triglycerides, and cholesterol as compared to the group 1, while group 3 demonstrated a significant statistical decrease. In contrast to groups 2 and 3, group 4exhibited a strong statistically significant decrease; nonetheless, there was no statistically significant difference between it and group 1.

Group 2 demonstrated a statistically significant decrease in serum HDL levels when compared to group 1, but group 3 showed a statistically significant rise when compared to group 2. There was no statistically significant difference between group 4 and group 1, however there was a large statistically significant increase when compared to groups 2 and 3.

Histopathological results

Only the result for subgroup Ia was shown because the histopathological findings of the control subgroups (Ia, Ib, and Ic) were nearly identical.

H&E results: (plate I, II)

Examination of H&E-stained sections of the liver of the control group revealed that the general architecture was formed of polygonal hepatocytes radiating from central vein with rounded vesicular nuclei and acidophilic cytoplasm. Blood sinusoids were seen in between adjacent hepatocytes **(Figure 1a)**. Portal area showed containing bile duct and hepatic artery **(Figure 2a).**

Examination of the FL group sections showed mononuclear inflammatory cells infiltration around dilated central vein. It was surrounded by degenerated hepatocytes with darkly stained nuclei. Some hepatocytes had deeply acidophilic cytoplasm. Dilated blood sinusoids with Kupffer cells were also seen **(Figure 1b; 2b).** Portal areas appeared with dilatation in the blood vessels, cellular infiltration, and bile duct proliferation. Hepatocytes were seen with vacuolated cytoplasm **(Figure 2b).**

The FL-Silymarin group examination showed many hepatocytes with deeply acidophilic cytoplasm and darkly stained nuclei that are radiating from congested dilated central vein and separated by blood sinusoids. Some hepatocytes still had vacuolated cytoplasm **(Figure 1c; 2c).** The portal area appeared to contain blood vessels with mononuclear inflammatory cells infiltration around. Some hepatocytes appeared with acidophilic cytoplasm and vesicular nuclei, while others still had vacuolated cytoplasm **(Figure 2c).**

The FL-MSC-CM group exhibited normal hepatocytes arranged in cords radiating from central vein, while few hepatocytes appeared with darkly stained nuclei, many of them were binucleated. Kupffer cells were seen inside blood sinusoids **(Figure 1d; 2d).** The portal area appeared with mild mononuclear inflammatory cells infiltration. Kupffer cells were also observed **(Figure 2d).**

Mallory's trichrome stain results: (plate III Figure 3)

Mallory's trichrome stained sections of the liver of

rats in the study groups revealed that the group 1 sections had few collagen fibers around the blood vessels of the portal area **(Figure 3a).** FL group sections showed dense collagen deposition around the blood vessels in portal area **(Figure 3b).** The FL – Silymarin group revealed moderate collagen fibers around the dilated vessels of portal area **(Figure 3c).** FL-MSC-CM group revealed minimal amount of collagen fibers around the blood vessels of portal area **(Figure 3d).**

Osmic acid stain results (plate III Figure 4):
Osmic acid-stained sections of the liver of rats in the study groups showed that the cytoplasm of the hepatocytes in the control group contained few lipid droplets **(Figure 4a).** FL group showed many lipid droplets of variable sizes in the cytoplasm of the hepatocytes **(Figure 4b).** FL – Silymarin revealed lipid droplets of variable sizes in the cytoplasm of the hepatocytes **(Figure 4c).** FL-MSC-CM group showed few lipid droplets in the cytoplasm of the hepatocytes **(Figure 4d).**

Immunohistochemical staining for alpha smooth muscle actin results (α-SMA): (plate IV Figure 5)
Immunohistochemical stained sections of the liver of rats in the study groups showed weak positive immunoreactivity in the wall of the vessels of portal area and blood sinusoids **(Figure 5a).** In the FL group strong positive immunoreaction in the wall of the vessels of portal area and blood sinusoids **(Figure 5b).** The FL – Silymarin group revealed moderate positive immunoreactivity in the wall of the vessels of portal area and blood sinusoids **(Figure 5c).** The FL-MSC-CM group showed weak positive immunoreactivity in in the wall of the vessels of portal area **(Figure 5d).**

Immunohistochemical staining for caspase 3 results: (plate IV Figure 6)
Immunohistochemical stained sections of the liver of rats in the study groups showed faint positive immunoreactivity in cytoplasm of the hepatocytes in the control group **(Figure 6a)**. In the FL group strong positive immunoreaction in cytoplasm of most hepatocytes was observed **(Figure 6b).** The FL – Silymarin group revealed moderate positive immunoreactivity on the cytoplasm of some hepatocytes **(Figure 6c)**. The FL-MSC-CM group showed weak positive immunoreactivity in cytoplasm of few hepatocytes **(Figure 6d).**

Ultrastructural results: (plate V, VI)
TEM examination of ultrathin sections from the liver of control group revealed hepatocytes with euchromatic nuclei. The cytoplasm contained mitochondria, rough endoplasmic reticulum, and smooth endoplasmic reticulum. Bile canaliculi can be seen in between hepatocytes **(Figure 7a; 8a).** Also, there were short microvilli protruding from the surface of hepatocytes into space of Disse **(Figure 8a).**
Electron microscopic examination of the FL group sections revealed hepatic nuclei with condensed peripheral heterochromatin, rarefied cytoplasm, mitochondria, and rough endoplasmic reticulum. Bundles of collagen were also seen **(Figure 7b)**. Multiple lipid droplets of variable sizes were also observed in the hepatocyte cytoplasm **(Figure 7c; 8b).** The blood sinusoids appeared with Kupffer cells, many red blood cells **(Figure 8b)**, multiple inflammatory cells, and Ito cells **(Figure 8c)**. Short, microvilli protruding into the space of Disse were also seen **(Figure 8c)**.
Examination of ultrathin sections of FL-Silymarin group showed hepatocytes nuclei with areas of peripheral heterochromatin and widening of nuclear envelope. The cytoplasm appeared contained some lipid droplet and dilated cisternae of rough endoplasmic reticulum **(Figure 7d).** Other hepatocytes appeared with euchromatic nuclei and prominent nucleoli. Blood canaliculi blood sinusoids were observed. Cytoplasm shows multiple small vacuoles **(Figure 8d).**
Ultra-thin sections examination of the FL-MSC-CM group exhibited adjacent hepatocytes with euchromatic nuclei. Mitochondria, rough endoplasmic reticulum, and smooth endoplasmic reticulum were seen in their cytoplasm **(Figure 7e).** The blood sinusoids appeared with sinusoidal endothelial cells, and telocytes in their lumen. Numerous microvilli occupying the perisinusoidal hepatic spaces were also seen **(Figure 8e).**

Morphometrical results (Figure 2s; Table 1):
Area % of α-SMA and caspase 3 immune reaction: There was statistically significant difference between the four studied groups regarding the area % of α-SMA and caspase 3 immune reaction with the highest level in group 2 and the lowest level in group 1. Group 3 was statistically lower than group 2. Group 4 showed a high statistically significant decrease than group 2 and group 3 with no statistically significant difference between it and group 1.

Table (1): Mean values (± SD) of liver index, lipid profile and morphometrical analysis in the studied groups:

	Control group	FL group	FL-silymarin group	FL-MSCs-CM group			
Groups	**Mean ± SD**	**Mean ± SD**	**Mean ± SD**	**Mean ± SD**	**F-Test**	**p-value**	**LSD**
1a) Liver index	2.65 ± 0.072	4.01 ± 0.047	3.93± 0.07	2.69 ± 0.14	681.407	<0.001**	
1b) Lipid profile							
Total cholesterol	53.37 ± 0.71	85.396 ± 2.64	81.91 ± 3.32	54.98 ± 0.58	486.661	<0.001**	0.001 **(a) 0.001** (b) 0.58(c) 0.05* (d) 0.001* *(e) 0.001** (f)
Serum triglycerides	82.02 ± 1.39	181.94 ± 5.33	176.84 ± 2.55	84.88 ± 1.37	1912.132	<0.001**	0.001 **(a) 0.001** (b) 0.48(c) 0.05* (d) 0.001* *(e) 0.001** (f)
Serum HDL	39.41 ± 0.76	14.88 ± 3.66 (9.45-20.12)	21.92 ± 6.33	38.01 ± 1.45	84.12	<0.001**	0.001 **(a) 0.001** (b) 0.45(c) 0.001** (d) 0.001* *(e) 0.001** (f)
Serum LDL	60.51 ± 3.63	126.32 ± 3.67	119.23 ± 2.99	62.96 ± 2.32	977.55	<0.001**	0.001 **(a) 0.001** (b) 0.12(c) 0.001** (d) 0.001* *(e) 0.001** (f)
1c) Morphometrical Analysis							
Mean area% of α-SMA	2.43 ± 0.72	11.39 ±2.12	5.75±1.33	2.76 ±0.93	152.91	<0.001**	
Mean area% of caspase 3	0.34 ± 0.07	36.33 ± 4.65	32.16 ± 4.84	0.48 ± 0.024	271.52	<0.001**	

One way ANOVA test LSD (least significant difference), Significant difference (p value ≤ 0.05), **Highly significant difference (p value ≤ 0.001), (a) group 1 versus group 2, (b) group 1 versus group 3, (c) group 1 versus group 4, (d) group 2 versus group 3, (e) group 3 versus group 4, (f) group 3 versus group 4.

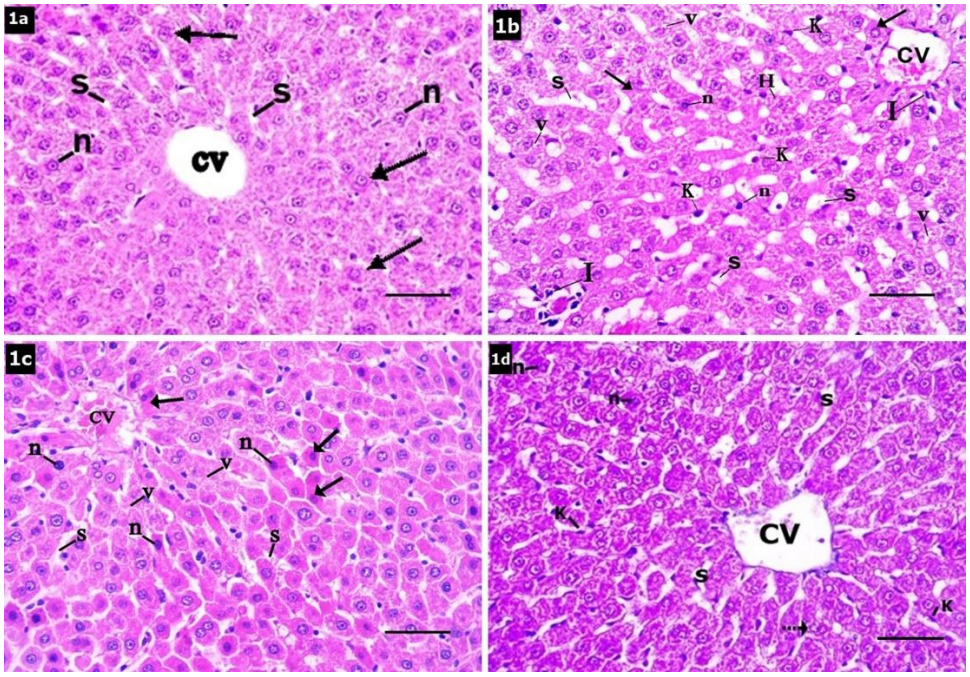

Plate I

Figure (1): Photomicrograph of sections stained by H&E of rat's liver: **(a) The control group** showing polygonal hepatocytes (arrows) radiating from central vein (CV) with rounded vesicular nuclei (n) and acidophilic cytoplasm. Blood sinusoids (s) are seen in between adjacent hepatocytes. **(b) FL group** reveals mononuclear inflammatory cells infiltration (I). Dilated central vein (CV) surrounded by degenerated hepatocytes (H) with darkly stained nuclei (n). Some hepatocytes have deeply acidophilic cytoplasm (arrow). Dilated blood sinusoids (s) and Kupffer cells (K) are also noticed. In **(c) FL – Silymarin group,** many hepatocytes with deeply acidophilic cytoplasm (arrows) and darkly stained nuclei are seen (n) radiating from the dilated congested central vein (CV) and separated by blood sinusoids (s). Some hepatocytes still have vacuolated cytoplasm (v). **(d) FL-MSC-CM group** showing apparent normal hepatocytes arranged in cords and radiating from central vein (CV). Few hepatocytes with darkly stained nuclei (n) are seen and many cells are binucleated (dotted arrows). Kupffer cells (K) are seen inside blood sinusoids (s). (H&E X400, scale bar 30 µm).

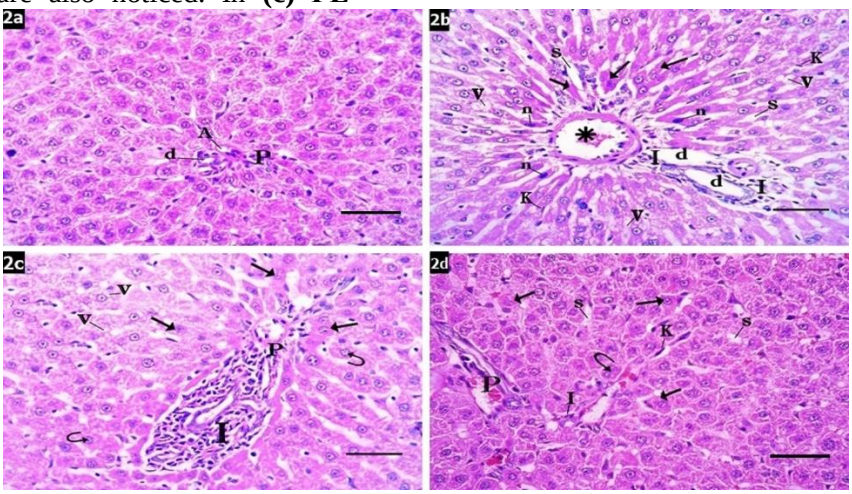

Plate II

Figure (2): Photomicrograph of sections stained by H&E of rat's liver: **(a) The control group** showing portal area (P) containing hepatic artery (A) and bile duct (D). **(b) FL group** showing congested (*) blood vessel, cellular infiltration (I) around portal area with bile duct proliferation (d). Hepatocytes with deep acidophilic cytoplasm (arrows) and darkly stained nuclei (n) are observed, while others appear vacuolated (v). Dilated Blood sinusoids (s) and

Kupffer cells (K) are also noticed. **(c) FL- Silymarin group** showing portal area (P) with cellular infiltration (I). Some hepatocytes appear with acidophilic cytoplasm (arrows) and vesicular nuclei (curved arrows) while others still have vacuolated cytoplasm (v). **(d) FL-MSC-CM group** showing mild mononuclear inflammatory cells infiltration (I) around portal area (P). Apparent normal hepatocytes with acidophilic (arrows) cytoplasm and vesicular nuclei are seen, some of them are binucleated (curved arrow). Also, there is few dilated sinusoids (s) and Kupffer cells (K). (H&E X400, scale bar 30 µm).

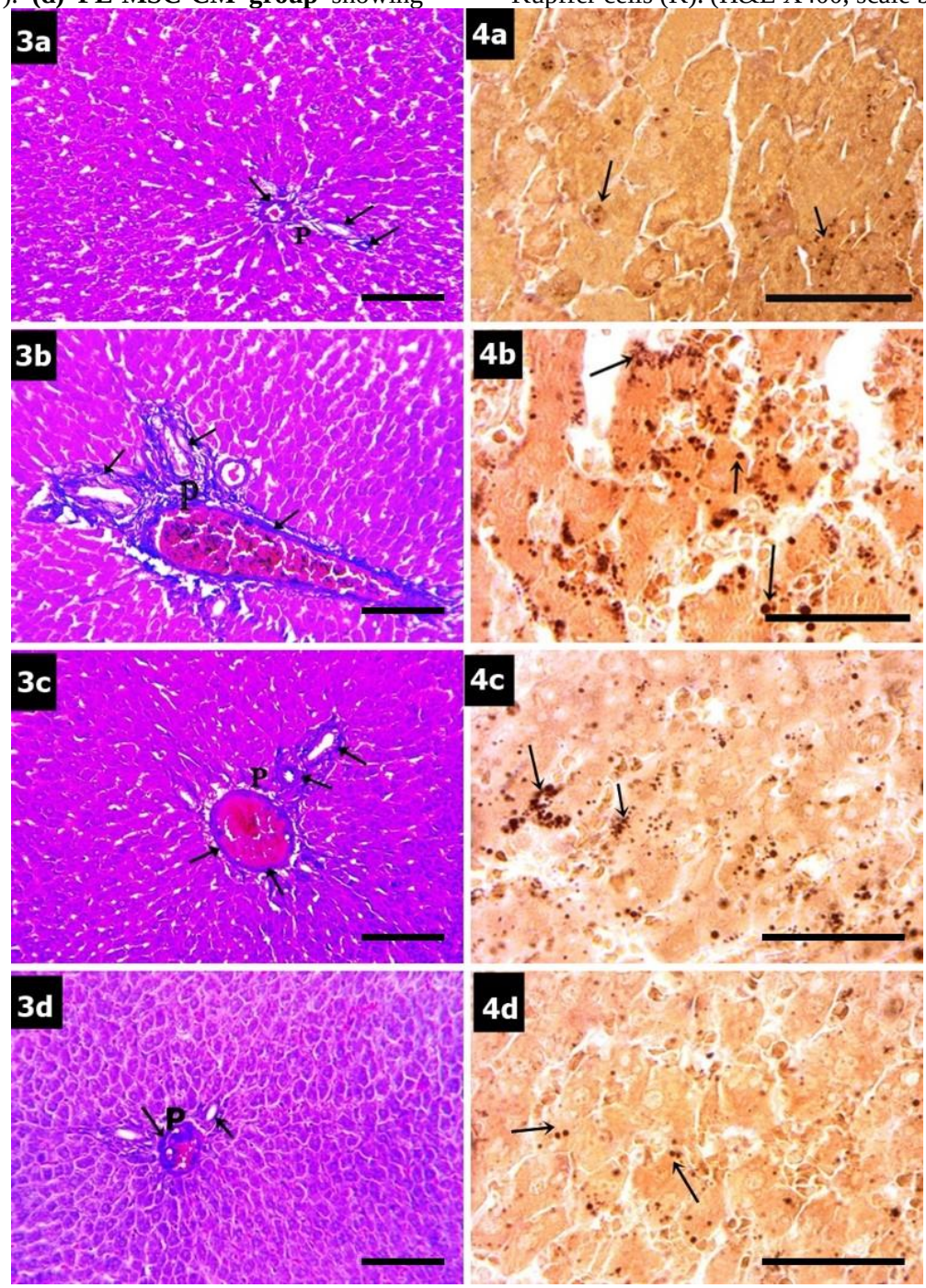

Plate III

Figure (3): Photomicrograph of sections stained by Mallory's trichrome of rats' liver **(a) The control group** showing few collagen fibers (arrows) around blood vessels of the portal area (P). (**b) FL group** reveals dense collagen deposition (arrows) around blood vessels in portal area (P). **(c) FL – Silymarin group** showing few collagen fibers (arrows) around the dilated vessels of portal area (P). In **(d) FL-MSC-CM group**, minimal amount of collagen fibers

(arrows) is seen around the vessels of portal area (P). (Mallory's trichrome x200, scale bar 30 µm).

Figure (4): Photomicrograph of sections stained by osmic acid of rats' liver. In the hepatocytes' cytoplasm, **(a) the control group** reveals a few lipid droplets (arrows), **(b) FL group** reveals many scattered lipid droplets of variable sizes (arrows), **(c) FL – Silymarin group** reveals scattered lipid droplets of variable sizes (arrows), however, in **(d) FL-MSC-CM group** few lipid droplets (arrows) are noticed. (Osmic acid x1000, scale bar 30 µm).

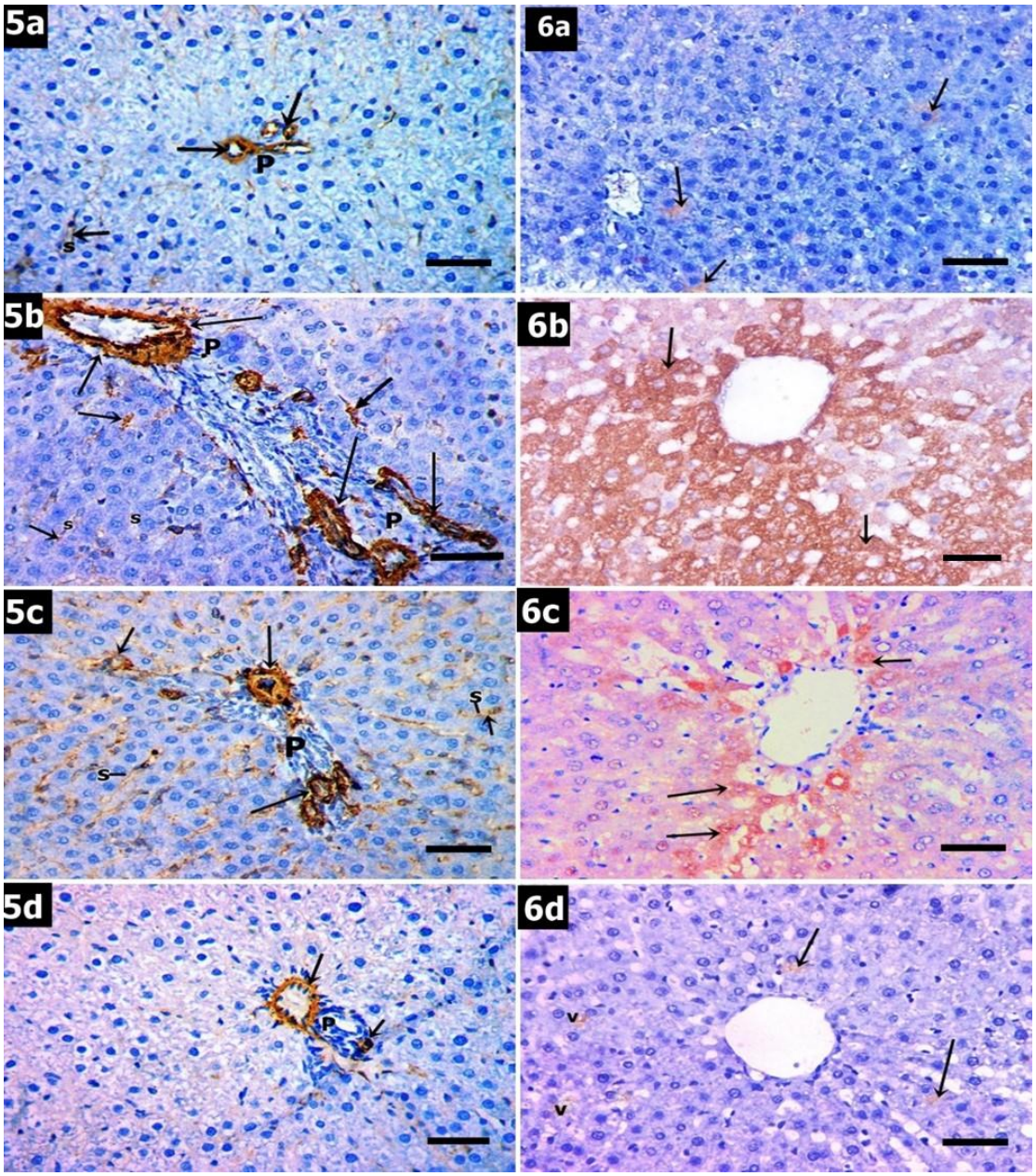

Plate IV

Figure (5): Photomicrograph of sections stained by α-SMA of rats' liver. In the wall of vessels of portal area (P) and blood sinusoids (s), **(a) The control group** shows weak positive immunoreaction (arrows), **(b) FL group** reveals strong positive immunoreaction (arrows), **(c) FL – Silymarin group** reveals moderate positive immunoreaction (arrows). **(d) FL-MSC-CM group** shows weak positive immunoreaction (arrows) in the wall of vessels of portal area (P). (Immunoperoxidase technique for α-SMA, X 400, scale bar 30 µm).

Figure (6): Photomicrograph of sections stained by caspase 3 of rats' liver. **(a) The control group** showing faint positive immunoreactivity (arrows) in hepatocytes' cytoplasm. **(b) FL group** reveals strong

positive immunoreaction for caspase 3 (arrows) in most hepatocytes' cytoplasm. **(c) FL – Silymarin group** reveals moderate positive immunoreaction (arrows) in some hepatocytes' cytoplasm. While in **(d) FL-MSC-CM group** weak positive immunoreaction (arrows) in few hepatocytes' cytoplasm is observed. (Immunoperoxidase technique for caspase 3, X 400, scale bar 30 µm).

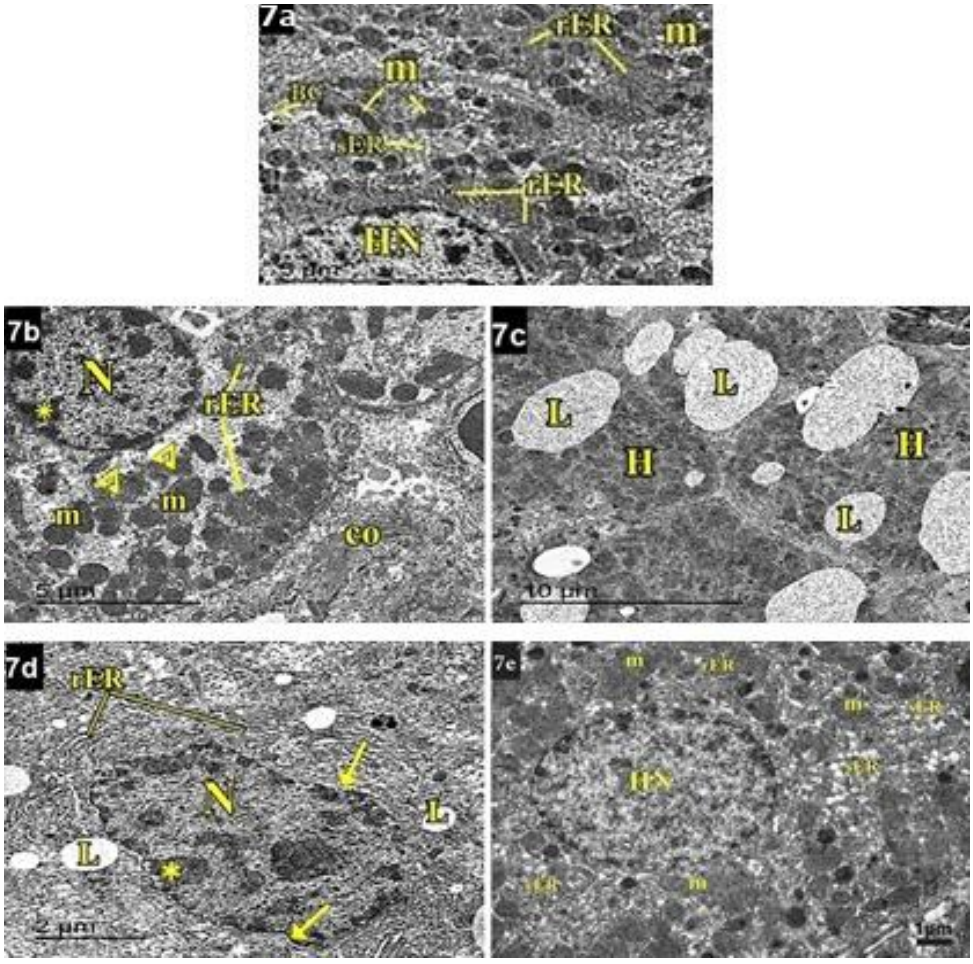

Plate V

Figure (7): Electron Photomicrographs of rats' liver. **(a) The control group** showing hepatocyte with euchromatic nucleus (HN). The cytoplasm has mitochondria (m), rough endoplasmic reticulum (rER) and smooth endoplasmic reticulum (sER). Bile canaliculus (BC) is observed in between hepatocytes (TEM X 13000). **(b) and (c) FL group showing in (b)** hepatocyte nucleus (N) with peripheral heterochromatin condensation (*). Rarified cytoplasm (arrow heads), mitochondria (m) and rough endoplasmic reticulum (rER) are observed. Bundles of collagen (co) are also noticed (TEM X 11000), and in **(c)** multiple lipid droplets (L) of variable sizes are seen in cytoplasm of hepatocyte (H) (TEM X 7000). **(d) FL – Silymarin group** showing hepatocyte with nucleus (N) contained peripheral condensation of heterochromatin (*). Widening (arrows) in the nuclear envelope is also noticed. The cytoplasm has a few lipid droplets (L) and dilated cisternae of rough endoplasmic reticulum (rER) (TEM X 17500). **(e) FL-MSC-CM group** showing hepatocyte with euchromatic nucleus (HN), mitochondria (m), rough endoplasmic reticulum (rER), smooth endoplasmic reticulum (sER) (TEM X 12300).

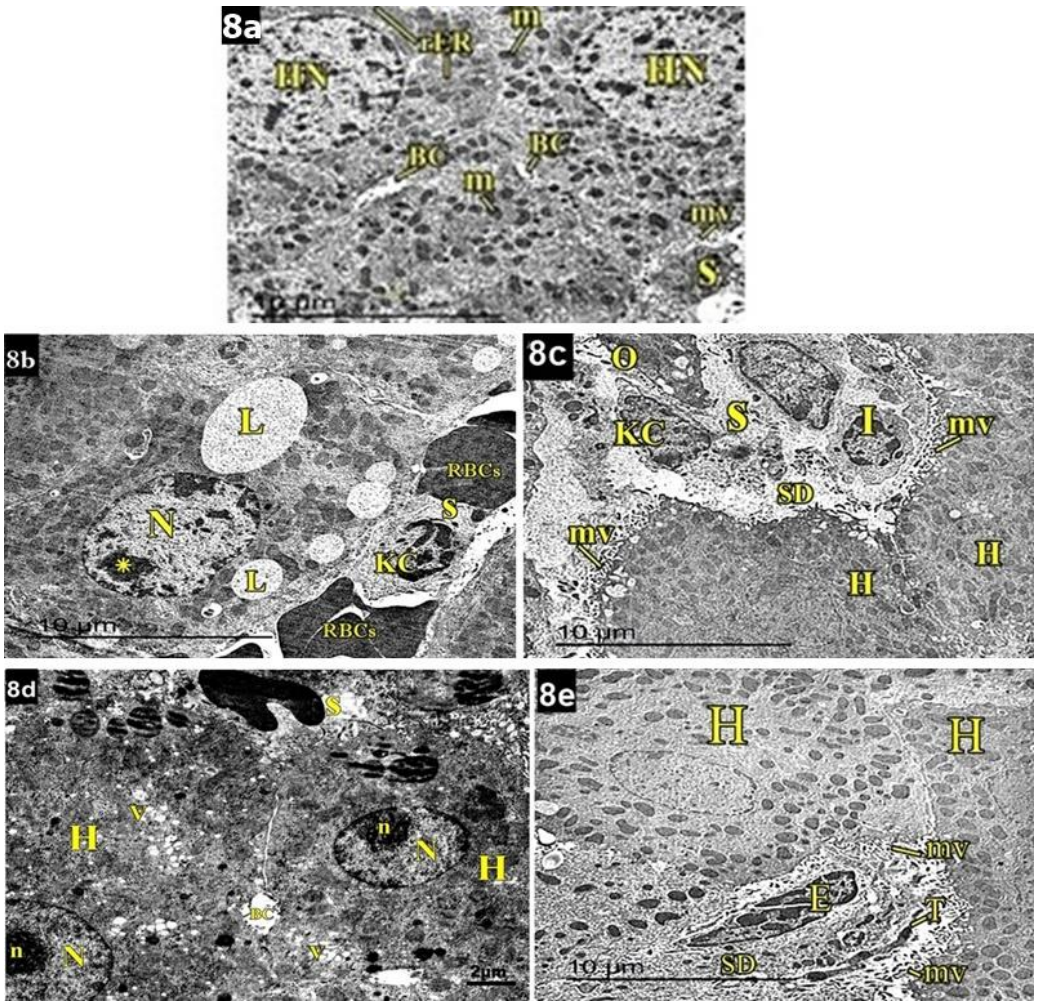

Plate VI

Figure (8): Electron Photomicrographs of rats' liver. **(a) The control group** shows adjacent hepatocytes with euchromatic nuclei (HN), mitochondria (m) and rough endoplasmic reticulum (rER). Bile canaliculi (BC) are seen in between hepatocytes. Short microvilli (mv) are noticed protruding from the surface of hepatocytes into space of Disse (s) (TEM X 7000). **(b) and (c) FL group** shows in **(b)** Blood sinusoid (s) contained Kupffer cell (Kc) and many red blood cells (RBCs) are seen. Hepatocytes are noticed with nucleus (N) that has peripheral heterochromatin condensation (*) and lipid droplets (L) in its cytoplasm (TEM X 7000), and in **(c)** multiple inflammatory cells (I), Kupffer cell (Kc) and Ito cell (O) in blood sinusoid (s). Short microvilli (mv) of adjacent hepatocytes (H) protruding into the space of Disse (SD) are noticed (TEM X 7000). **(d) FL– Silymarin group** showing adjacent hepatocytes (H) with euchromatic nuclei (N) and prominent nucleoli (n). Blood canaliculus (BC) and blood sinusoid (s) are observed. Cytoplasm shows multiple small vacuoles (V). (TEM X 8700). In **(e) FL-MSC-CM group,** blood sinusoid (S) is seen with endothelial cell (E) and telocyte (T) in its lumen. Adjacent hepatocytes (H) with numerous microvilli (mv) occupying the perisinusoidal hepatic space (SD) are observed (TEM X 7000).

DISCUSSION

Data obtained from control subgroups (Ia, Ib, Ic) were approximately identical, so results of all were combined and represented as a single control group. This was supported by the findings of **Ramezannezhad et al.** and **Bahmani et al. [32, 33]** who reported that neither Silymarin nor conditioned media had an impact on normal liver.

The fatty liver (FL) group's body weights increased significantly in the current study when compared to the control group; this finding was consistent with **Cui et al. [34].** There is also significant increase in liver index in this group as compared to control group a result similar to **Yang et al. [35]** who attributed the

liver enlargement to the administration of high fat diet. According to **Salah Nour et al. [36]** the weight gain was due to increased calorie intake because it promotes a positive energy balance, which leads to weight gain and increased visceral fat deposition.

In current work, FL group showed a statistically significant rise in the mean values of the serum biochemical parameters (TC, TG, LDL) and decreased level of HDL as compared to control group. These findings were in agreement with the reports of **Habib et al. [37]** who concluded that a high-fat diet was a successful means of inducing obesity.

Ma et al, [38] added that excess FFA accumulation by high lipid diet beyond the hepatic mitochondria's oxidative capacity resulted in an abundance of TG released into the blood stream, raising serum levels of TG, TC, and LDL**.**

In current work light microscopic examination of FL group hepatocytes appeared degenerated with vacuolated cytoplasm and fading nuclei, others had deeply acidophilic cytoplasm and darkly stained nuclei. These results were in agreement with **Habib et al. [37]**.There are two types of hepatocellular steatosis: (first type is the macrovesicular type where the hepatocytes have well-defined fat vacuoles that can push the nucleus to the periphery, while the second type is the microvesicular one where the hepatocytes contain small fat vacuoles in the cytoplasm with the nucleus located centrally).The hepatic steatosis is caused by lipogenic genes activation that transcript fatty acid synthase (FAS) and other sterol regulatory elements resulting in excessive increase in triglycerides and fatty acids in the liver **[39, 40].**

Deep acidophilic cytoplasm was also found by **Leow et al., [41]** who stated that these acidophilia which were detectable under light microscope may be due to enlarged mitochondria, or megamitochondria, as eosinophilic inclusions in the cytoplasm or due to (acidophilic bodies) which result from apoptosis of hepatocytes according to the severity of inflammation.

In the present study, some hepatocytes had dark pyknotic nuclei, which were verified by chromatin condensation, this result was confirmed statistically by significant increase in the expression of caspase-3 in FL group and was similar to what was found by **Dwivedi and Jena, [42]. Hosny et al, [43]** attributed this result of reduced antioxidant activity that leaves cells more susceptible to the damaging effects of reactive oxygen species. Also, they added that some cells exhibited vacuolated nuclei, known as glycogenated nuclei, as a result of the buildup of glycogen in the nucleus which can be seen in liver biopsies from individuals with (NAFLD), Wilson disease and diabetes.

In current work, there were many mononuclear inflammatory cells infiltration in between hepatocytes in FL group. The portal area of the same group also showed mononuclear cellular infiltration**,** bile duct proliferation, and congested portal vessels. These results were in agreement with **Habib et al.; Ibrahim et al.** and **Kundu et al. [37, 44, 45]. Hegazy et al. [46]** reported that the development of portal hypertension is responsible for the dilatation and congestion of the portal vein as large, ballooned hepatocytes compress the blood sinusoids, causing them to constrict and raising intrahepatic vascular resistance.

An et al, [47] suggested that portal-based alterations, such as ductular reaction (DR), a reactive lesion consisting of tiny biliary ductules and an associated complex of inflammatory cells and stroma, are linked to portal inflammation. Hepatic progenitor cells (HPCs) stimulate a secondary proliferation pathway in response to necrotic and apoptotic hepatocyte replacement, which is the fundamental mechanism of (DR). Under normal circumstances, the neighbouring hepatocytes within the lobules replicate, maintaining the principal route of liver regeneration. When the first system is damaged by toxins, viruses or alcohol, the secondary pathway takes over and HPCs multiply and differentiate into bile ductal epithelia and hepatocytes, with the DR as a by-product.

Mallory's trichrome stained sections of the fatty liver treated in this study showed a noticeable increase in collagen fibers surrounding the blood vessels. This result was consistent with the findings of **Fathy et al. [48]**. Also, in our work strong positive α-SMA immunoreactions was detected in media of the portal blood vessels. Morphometrical and statistical analysis supported this, and it was consistent with the findings of **Hany et al. [49]** who reported that HSCs are the primary mediators of regeneration. Extracellular matrix deposition is caused by the induction of fibrillary collagens and α-SMA by HSC activation.

Since alpha-smooth muscle actin (α-SMA) is frequently utilized to identify pathologic fibroblasts, it was employed as a marker for the identification of hepatic stellate cell activity. During liver damage and wound healing, α-SMA levels increase in HSCs as they transform into myofibroblasts **[27, 50, 51]**.

The presence of hepatic stellate cells (Ito cells) was confirmed by its presence in the electron microscopic examination.

In the current work, osmic acid staining of the same group revealed multiple lipid droplets inside cytoplasm of hepatocytes.

Ultrathin sections examination of FL group showed bundles of collagen, irregular hepatocytes with condensed heterochromatic nuclei, swollen mitochondria, dilated rough endoplasmic reticulum, numerous microvilli and areas of rarefied cytoplasm and blood sinusoid with many inflammatory cells which confirmed light microscopic findings, similar results were obtained by **Abo El-khair et al.; Kandeal et al.** and **Sorour et al. [52-54]. Abo El-khair et al. [52]** stated that endoplasmic reticulum (ER) stress may play a key role in the pathophysiology of NAFLD, as it is connected with both misfolded protein synthesis and oxidative damage. Both are related variables that may affect lipid metabolism and triglyceride accumulation within hepatocytes. Furthermore, ER stress can accelerate triglyceride and cholesterol production and intrahepatocyte accumulation while inhibiting lipoprotein secretion.

Additionally, **Zineldeen et al. [55]** noted that a calcium ion imbalance can lead to mitochondrial malfunction by disrupting the precise signalling between the mitochondria and the ER, a condition that is observed in a number of neurological and metabolic disorders.

The increased microvilli in the space of Disse and pericellular spaces may provide protection against metabolic demands caused by low oxygen pressure, increased collagen synthesis, or poor substrate diffusion from sinusoids due to changes in the space of Disse according to **Ahishali et al. [56]**.

In the present work, there was a significant decrease in liver weights of the Silymarin group compared to FL group. This observation was in accordance with **El-Desoky et al. [57]** who added that Silymarin anti-inflammatory effect was due to the reduction of tumor necrotic factor- α (TNF-α) pro-inflammatory cytokine, it also reduced Malondialdehyde (MDA) significantly as an antioxidant effect.

In current work, administration of Silymarin showed a significant decrease in serum levels of TG, TC, and LDL and increase in HDL. This was in accordance with **Guo et al. [58]** and **Doostkam et al. [59]** who stated that improvement in Silymarin group occurred not only due to significant antioxidant activity, as demonstrated by increased SOD and reduced MDA, but also due to an increase in irisin (a newly discovered polypeptide), anti-inflammatory and antifibrotic activities. **Kalopitas et al. [60]** also said that Silymarin exhibited antioxidant characteristics by stimulating polymerase and RNA transcription, protecting the cell membrane from radical damage, and inhibiting toxin absorption.

In the current work, H and E-stained liver sections of the Silymarin group showed variable degrees of improvement. Some lobules showed hepatocytes with normal lobular architecture while other areas showed loss of lobular architecture. Similar findings were described by **Doostkam et al. [59]** who reported that Silymarin treated type 2 diabetic rats showed changed hepatic lobules with fat accumulation inside the cytoplasm and some lymphocyte infiltration. The electron microscopic examination of the same group confirmed the light microscopic findings.

The following mechanisms explain how Silymarin works: it scavenges free radicals, regulates both enzymatic and non-enzymatic antioxidant responses by controlling transcription factors nuclear related factor 2, which is the coordinator of the antioxidant and cytoprotective response, and another factor involved in the inflammatory process which is nuclear factor-Kappa β. Silymarin inhibits free radical production by inducing the gene expression of protector substances as sirtuins and heat shock proteins and suppressing the producer enzymes providing protection against oxidative stress **[61].**

Regarding Mallory's trichrome staining of the same group few collagen fibers were detected around the portal area.

According to **Doostkam et al. [59],** Silymarin exhibits encouraging antifibrotic properties in liver injury models. By increasing glutathione levels, it lessens oxidative stress. By reducing leukotrienes, inhibiting the lipo-oxygenase cycle, and enhancing Kupffer cell activity in rats, Silymarin may lessen hepatic inflammation.

In the present work, osmic acid staining of the same group revealed less lipid droplets inside cytoplasm of hepatocytes than FL group.

Silymarin-treated group showed positive α-SMA immunoreaction in the wall of vessels of portal area. This reaction showed a significant statistical difference when compared to FL group that was confirmed morphometrically. Our result was similar to **Wang et al. [62]** who reported that Silymarin effect on a liver fibrosis model has decreased the number of α-SMA positive cells.

In the same group positive caspase immunoreaction was detected in cytoplasm of the hepatocytes that was statistically lower than FL group. **Yassin et al. [63]** stated that the anti-apoptotic effect of Silymarin may occur through modulation of oxidative stress-induced apoptosis by increasing the expression of B-cell leukaemia/lymphoma 2 protein (Bcl-2) and decreasing the levels of Tumour protein P53 (p53) and cleaved-caspase-3 expressions on a rat model of renal carcinoma.

However, Silymarin has many advantages and showed some significant improvement, but **Zhang et al. [64]** reported that the bulk of Silymarin's components have physicochemical characteristics, such as limited oral bioavailability, poor solubility, or chemical instability, that restrict their bioactivities.

There was a significant decrease in liver index in the conditioned media group when compared to FL and Silymarin groups with non-significant difference between it and control group.

In current work, the conditioned media group showed significant improvement in lipid profile with a marked elevation in HDL levels together with significantly decreased levels of TC, TG, LDL. Our result was similar to **Elshemy et al. [65] and Tan et al. [66]. Elshemy et al. [65]** found that adipose-mesenchymal stem cells conditioned media significantly decreased TC, TG, LDL, and total lipids with a marked elevation in HDL levels in type 2 diabetic rats.

In the current work, H&E-stained sections of the conditioned media group showed restoration of general hepatic lobular architecture with less cellular infiltration and some cells are still vacuolated. Our results were similar to **Ravan et al. [67]** who found that human umbilical cord-mesenchymal stem cells conditioned medium had the same effect on a rat model of liver fibrosis and they attributed this to the anti-oxidative, anti-fibrotic and anti-inflammatory effects of this agent.

Also, **Ravan et al. [67]** added that the antifibrotic effect of conditioned media was due to inhibition of the production of the transforming growth factor- b1 (TGF-b1) gene and its receptor TGF-β receptor type 2 (TbRII).

Ra et al. [68] confirmed the antioxidant effect of human adipose stem cell conditioned medium by enhancing the growth and implantation of mice embryos in vivo and they attributed this to upregulation of antioxidant gene expression in the reproductive organs.

Jin et al. [69] reported that the anti-inflammatory effect of mesenchymal stem cells conditioned media was due to the inhibitory effect of the mRNA transcription of pro-inflammatory chemokine receptors, chemokines, and cytokines in the lipopolysaccharide (LPS)-stimulated macrophages using reverse transcription polymerase chain reaction analysis, and also to the reduction of the production of the proteins like cyclooxygenase-2 (COX-2) and inducible nitric oxide synthase (iNOS) in LPS-activated macrophage when treated with (MSC-CM) stimulated with interleukin 4.

Yang et al. [8] found that MSC-CM could improve the biological activities of mitochondria, lowering inflammatory responses, and preventing cell death in T2DM models both in vivo and in vitro, and they referred these effects to the upregulation of Sirt 1.

In this study, osmic acid staining of the same group revealed only few lipid droplets inside cytoplasm of hepatocytes similar to control group.

There was few collagen deposition and weak positive immune reaction to α-SMA in the same group that was confirmed by statistical analysis which showed no statistically significant difference in area percentage of α-SMA when compared to control group. Our result was similar to **Ravan et al. [67]** who reported that human umbilical cord (MSCs-CM) had the same effect on a rat model of chronic liver fibrosis.

This decrease of collagen fibers in our study is due to the conditioned media anti fibrotic effect as mentioned before, also **Laksmitawati et al. [70]** stated that topical usage of conditioned media had decreased collagen content in burns leading to better scarring and they attributed this to the conditioned media paracrine effect.

In the current work, the conditioned media group showed weak positive immune reaction for caspase 3, a result that was confirmed statistically and was similar to **Squecco et al. [71]** who used the conditioned media in a rat model of myopathy and reported that because of the inhibitory effect of the media against activated mitochondria-dependent caspase 3 pathway, caspase 3 expression decreased.

The production of paracrine angiogenic factors such as VEGF (vascular endothelial growth factor) and HGF (hepatocyte growth factor) and can increase vascularization and engage in cell regeneration while also reducing the apoptotic rate by lowering caspase-3 activity in islet cells of pancreas following MSC-CM **[65].**

In our study, ultrathin sections examination of the same group confirmed the light microscopic findings. Hepatocytes appeared with euchromatic nuclei, mitochondria, rough endoplasmic reticulum, smooth endoplasmic reticulum, and glycogen granules. Blood sinusoid appeared with sinusoidal endothelial cells, Kupffer cells and telocytes in its lumen with microvilli occupy the perisinusoidal hepatic space. Bile canaliculi were also seen between adjacent hepatocytes.

Kupffer cells may play a part in liver regeneration, according to research by **Du et al. [72]** who found that mesenchymal stem cells conditioned media has not only reduced the hepatocyte apoptosis, but also improved its regeneration by significant reduction in neutrophil infiltration, significant decrease in pro

inflammatory cytokines level and Kupffer cells activation.

Recently discovered interstitial cells known as telocytes are distinguished by long, thin cytoplasmic extensions. They can exchange information with other cells via specialized junctions (cell/cell) or extracellular vesicle overflow. Indeed, growing research indicates a close connection between telocytes and stem cells inside tissues, which facilitates tissue repair and regeneration **[73].**

The provided findings showed that AD-MSCs reduce the chronic liver diseases development in animal models, including NAFLD, liver fibrosis, and cirrhosis, which may explain their wide therapeutic effectiveness in treating the liver diseases clinically. MSC-CM is used to treat diabetes and NAFLD as it can reduce insulin sensitivity and resistance in mice with type 2 diabetes, and also alleviating liver dysfunction, improving lipid profiles, decrease inflammation, decrease apoptosis and increase the antioxidant capability **[8, 74].**

Conclusions

The present study revealed MSCs-CM has a more ameliorative effect than Silymarin on induced fatty liver disease through its anti-necrotic, antiapoptotic and anti-inflammatory effects.

Conflict of interest

The authors declared that they have no conflicts of interest with respect to the authorship and/ or publication of this article.

Financial disclosures

This study was not supported by any source of funding.

REFERENCES

1. Loomba R, Friedman SL, Shulman GI. Mechanisms and disease consequences of nonalcoholic fatty liver disease. *Cell*, 2021; 184(10), 2537-64.
2. Pouwels S, Sakran N, Graham Y, Leal A, Pintar T, Yang W, et al. Non-alcoholic fatty liver disease (NAFLD): a review of pathophysiology, clinical management and effects of weight loss. *BMC Endocr Disord* 2022; 22(1), 1-9.
3. Lee KC, Wu PS, Lin HC. Pathogenesis and treatment of non-alcoholic steatohepatitis and its fibrosis. *Clin Mol Hepatol* 2023; 29(1), 77.
4. Huh Y, Cho YJ, Nam GE. Recent epidemiology and risk factors of nonalcoholic fatty liver disease. *J Obes Metab Syndr* 2022;31(1), 17.
5. Bellavite P, Fazio S, Affuso F. A Descriptive Review of the Action Mechanisms of Berberine, Quercetin and Silymarin on Insulin Resistance/Hyperinsulinemia and Cardiovascular Prevention. *Molecules* 2023; 28(11), 4491.
6. Ivanov V, Slavova V, Georgieva D, Petrova-Tacheva V, Tolekova A. Use of Silymarin for reducing nephrotoxicity caused by medicaments. *Bulg Chem Commun* 2020; 52:136-41.
7. Das R, Mitra S, Tareq AM, Emran TB, Hossain MJ, Alqahtani AM, et al. Medicinal plants used against hepatic disorders in Bangladesh: A comprehensive review. *J Ethnopharmacol* 2022; 282, 114588.
8. Yang M, Cui Y, Song J, Wang L, Liang K, Sha S, et al. Mesenchymal Stem Cell Conditioned Medium Improves Non-alcoholic Fatty Liver Disease in Type 2 Diabetic Mice by Regulating SIRT1. *Biochem Biophys Res Commun* 2021; 546:74-82.
9. Ibrahim R, Mndlovu H, Kumar P, Adeyemi SA, Choonara YE. Cell Secretome Strategies for Controlled Drug Delivery and Wound-Healing Applications. *Polymers*, 2022; 14(14), 2929.
10. Omage SO, Orhue NE, Omage K. Dennettia tripetala Relieves Chronic Hepatorenal Injuries in Rats by Altering fas, sod-1, and tnf-α Expression. *Prev Nutr Food Sci* 2022; 27(1), 89.
11. Hashemi SM, Hassan ZM, Hossein-Khannazer N, Pourfathollah AA, Soudi S. Investigating the route of administration and efficacy of adipose tissue-derived mesenchymal stem cells and conditioned medium in type 1 diabetic mice. *Inflammopharmacol*, 2020; 28, 585-601.
12. Abd Allah SH, Hussein S, Hasan MM, Deraz RH, Hussein WF, Sabik LM. Functional and Structural Assessment of the Effect of Human Umbilical Cord Blood Mesenchymal Stem Cells in Doxorubicin-Induced Cardiotoxicity. *J Cell Biochem* 2017; 118(10), 3119-29.
13. Pinheiro D, Dias I, Freire T, Thole AA, Stumbo AC, Cortez EAC, et al. Effects of mesenchymal stem cells conditioned medium treatment in mice with cholestatic liver fibrosis. *Life Sci* 2021; 281, 119768.
14. Saeed Abd El-Lateef AE, Abd Rabou Fayyad R, Mohamed Mohamed Algendy A. Comparative Effects of Olive Leaves Extract and Silymarin on Hepatic Redox State in Experimentally Carbon Tetrachloride-Induced Liver Injury in Adult Male Albino Rats. *Al-Azhar Med J* 2022; 51(2), 1311-24
15. Shuang CUI, Xiao-Jie P, Chao-Liang GE, Yi-Tong GUO, Zhang PF, Ting-Ting YAN, et al.

Silybin alleviates hepatic lipid accumulation in methionine-choline deficient diet-induced nonalcoholic fatty liver disease in mice via peroxisome proliferator-activated receptor α. *Chin J Nat Med* 2021; 19(6), 401-11.

16. Abdel-Aal S, Abdelrahman S, Raafat N. Comparative therapeutic effects of mesenchymal stem cells versus their conditioned media in alleviation of CCL4-induced liver fibrosis in rats: Histological and biochemical study. *J Med Histol* 2019; 3(1), 1-20

17. Asgari Taei A, Dargahi L, Khodabakhsh P, Kadivar M, Farahmandfar M. Hippocampal neuroprotection mediated by secretome of human mesenchymal stem cells against experimental stroke. *CNS Neurosci Ther* 2022; 28(9), 1425-38.

18. Bahmani M, Ziamajidi N, Hashemnia M, Abbasalipourkabir R. Human umbilical cord-derived mesenchymal stem cells conditioned medium ameliorates CCl4-induced liver fibrosis through regulation of expression and activity of liver lysyl oxidase. *Toxin Rev* 2021; 40(4), 971-84.

19. Banerjee A, Das D, Paul R, Roy S, Bhattacharjee A, Prasad SK, et al. Altered composition of high-lipid diet may generate reactive oxygen species by disturbing the balance of antioxidant and free radicals. *J Basic Clin Physiol Pharmacol* 2020; 31(3), 20190141

20. Zhang Q, Fan XY, Cao YJ, Zheng TT, Cheng WJ, Chen L J, et al. The beneficial effects of Lactobacillus brevis FZU0713-fermented Laminaria japonica on lipid metabolism and intestinal microbiota in hyperlipidemic rats fed with a high-fat diet. *Food Funct* 2021; 12(16), 7145-60.

21. Amir, Z, Asghar Z, Gholamreza S, Mehran H, Zoya T. Determining the Effect of Methadone on Lipid Profile, Serum Leptin, and Liver Enzymes Levels in Male and Female Rats. *Current Topics on Chemistry and Biochemistry* 2023; 8, 84-97.

22. Abdel-Halim KY, OsmanSR, Abuzeid MAF, Khozimy AM. Hematological Changes and Oxidative Stress Induction of Titanium Dioxide Nanoparticles in Male Mice after Intraperitoneal Injection of Different Doses for 28 Days: Study of Organ's Responsibility. *NanoWorld J*, 2021; 7(2), 22-32.

23. Ranjbar E, Tavakol Afshari J, KhajaviRad A, Ebrahimzadeh-Bideskan A, Shafieian R. Insights into the protective capacity of human dental pulp stem cells and its secretome in cisplatin-induced nephrotoxicity: effects on oxidative stress and histological changes. *J Basic Clinic Physiol Pharmacol* 2022; 34(3), 349-56.

24. Suvarna KS, Layton C, Bancroft JD. Bancroft's Theory and Practice of Histological Techniques E-Book. 8th ed., J Res Health Sci, 2018; China. 126-39; 434-75.

25. Wei LP, He FC, Chen XW, Lu SB, Marco L, Robbert DI. Osmic acid staining of myelin sheath in normal and regenerated peripheral nerves. Chin J Traumatol, 2007; 10(02): 86-9.

26. Abd-Elhafeez HH, Abou-Elhamd AS, Soliman SA. Morphological and immunohistochemical phenotype of TCs in the intestinal bulb of Grass carp and their potential role in intestinal immunity. *Sci Rep* 2020; 10(1), 14039.

27. Breuer DA, Pacheco MC, Washington MK, Montgomery SA, Hasty AH, Kennedy AJ. CD8+ T cells regulate liver injury in obesity-relatednonalcoholic fatty liver disease. *Am J Physiol Gastrointest Liver Physiol* 2020; 318(2): G211-24

28. Iyer AKV, Rojanasakul Y, Azad N. Nitrosothiol signaling and protein nitrosation in cell death. *Nitric oxide* 2014; 42: 9-18.

29. Ramos-Vara JA, Kiupel M, Baszler T, Bliven L, Brodersen B, Chelack B, et al. Suggested guidelines for immunohistochemical techniques in veterinary diagnostic laboratories. *J Vet Diagn Invest* 2008; 20(4): 393-413.

30. Tizro P, Choi C, Khanlou N. Sample preparation for transmission electron microscopy. In Biobanking, Methods and protocol, New York, *Humana press* 2019; 417-24

31. Abdi, H., & Williams, L. J. Tukey's honestly significant difference (HSD) test. *Encyclopedia of research design* 2010; 3(1), 1-5.

32. Ramezannezhad P, Nouri A, Heidarian E. Silymarin mitigates diclofenac-induced liver toxicity through inhibition of inflammation and oxidative stress in male rats. *J Herbmed Pharmacol 2019;* 8(3), 231-7.

33. Bahmani M, Ziamajidi N, Hashemnia M, Abbasalipourkabir R, Salehzadeh A. Human umbilical cord blood mesenchymal stem cell conditioned medium (hMSC-CM) improves antioxidant status in carbon tetrachloride-induced oxidative damage in rat. *Iran J Sci Technol Trans Sci* 2020; 44, 1327-35.

34. Cui H, Li Y, Wang Y, Jin L, Yang L, Wang L, et al. Da-chai-hu decoction ameliorates high fat diet-induced nonalcoholic fatty liver disease through remodeling the gut microbiota and

modulating the serum metabolism. *Front Pharmacol* 2020; 11, 584090.

35. Yang XX, Wang X, Shi TT, Dong JC, Li FJ, Zeng LX, et al. Mitochondrial dysfunction in high-fat diet-induced nonalcoholic fatty liver disease: The alleviating effect and its mechanism of Polygonatum kingianum. *Biomed Pharmacother* 2019; 117, 109083.

36. Salah Nour M, Sakara ZAEH, Hasanin NA, Hamed SM. Histological and immunohistochemical study of the effect of liraglutide in experimental model of non-alcoholic fatty liver disease. *Egyptian J Basic Appl Sci* 2023; 10(1), 342-57.

37. Habib M, Khalefa A, Alsemeh AE. Vitamin D3 protects against non-alcoholic fatty liver disease in rats by modulating hepatic iron deposition. *Egypt J Histol* 2023; 46(2), 832-46.

38. Ma B, Li P, An H, Song Z. Electroacupuncture attenuates liver inflammation in nonalcoholic fatty liver disease rats. *Inflammation* 2020; 43(6), 2372-8.

39. Abofila MT, Azab AE, Ali AN, Zohdy ED, Mohammed GF, Attia AM. Hepatic Histopathological Alterations induced by L-Arginine and/or Dexamethasone in Adult Male Albino Rats. *J Gastroenterol Hepatol*, 2022; 1-13

40. Florescu MM, Gheonea DI. Morphopathology of Nonalcoholic Fatty Liver Disease. In Essentials of Non-Alcoholic Fatty Liver Disease: Complications and Extrahepatic Manifestations. *Cham: Springer Sci Rev* 2023; 89-98.

41. Leow WQ, Chan AWH, Mendoza PGL, Lo R, Yap K, Kim H. Non-alcoholic fatty liver disease: the pathologist's perspective. *Clinical and Molecular Hepatology* 2023; 29: S302.

42. Dwivedi DK, Jena GB. NLRP3 inhibitor glibenclamide attenuates high-fat diet and streptozotocin-induced non-alcoholic fatty liver disease in rat: studies on oxidative stress, inflammation, DNA damage and insulin signalling pathway. *Naunyn-Schmiedeberg's Arch Pharmacol* 2020; 393(4), 705-16.

43. Hosny SA, Moustafa MHA, Mehina FM, Sabry MM. Therapeutic effect of autophagy induced by rapamycin versus intermittent fasting in animal model of fatty liver. *Folia Histochem Cytobiol* 2023; 61(4), 205-16.

44. Ibrahim SN, Saied NG, Hamam GG, Fawzy HM. Effect of Probiotics Versus Silymarin on a Model of Non-Alcoholic Fatty Liver in Adult Male Albino Rats. A Histological Study. *EAJBSD* 2023;15(2), 133-51.

45. Kundu D, Kennedy L, Zhou T, Ekser B, Meadows V, Sybenga A, et al. p16 INK4A drives nonalcoholic fatty liver disease phenotypes in high fat diet fed mice through biliary E2F1/FOXO1/IGF-1 signaling. *Hepatology* 2023; 78(1), 243-57.

46. Hegazy AA, Qenawy NM, Abdel Aziz NM, El-Bestawy EM. Possible Protective Role of Capsaicin Against High Fat Diet Effects on Liver and Gall Bladder of Adult Male Mice. *Egypt J Histol* 2021; 46(1): 245-62.

47. An L, Wirth U, Koch D, Schirren M, Drefs M, Koliogiannis D, et al. The role of gut-derived lipopolysaccharides and the intestinal barrier in fatty liver diseases. *J Gastrointest Surg* 2022; 1-13.

48. Fathy MA, Zamzam SA, Gergis NK, Hendy NE, Abdelfattah MT, Alsemeh AI. Adropin is Involved in the Ameliorative Effect of Chronic Exercise in Non-alcoholic Fatty Liver Rat Model. *Zagazig univ med j* 2023; *29*(4), 1071-85

49. Hany NM, Eissa S, Basyouni M, Hasanin AH, Aboul-Ela YM, Elmagd MA, et al. Modulation of hepatic stellate cells by Mutaflor® probiotic in non-alcoholic fatty liver disease management. *J Transl Med* 2022; 20(1), 1-19

50. Sun KH, Chang Y, Reed NI, Sheppard D. α-Smooth muscle actin is an inconsistent marker of fibroblasts responsible for force-dependent TGFβ activation or collagen production across multiple models of organ fibrosis. *Am J Physiol Lung Cell Mol Physiol* 2016; 310(9), 824-36.

51. Rockey DC, Du Q, Shi Z. Smooth muscle α-actin deficiency leads to decreased liver fibrosis via impaired cytoskeletal signaling in hepatic stellate cells. *Am J Pathol* 2019; 189(11): 2209-20.

52. Abo El-khair SM, Ghoneim FM, Shabaan DA, Elsamanoudy AZ. Molecular and ultrastructure study of endoplasmic reticulum stress in hepatic steatosis: Role of hepatocyte nuclear factor 4α and inflammatory mediators. *Histochem Cell Biol* 2020; 153, 49-62.

53. Kandeal HA, Eid FA, Abdelhafez H, El-Hady A, Mahmoud A. Role of Acacia arabica gum in reducing the impair alterations in liver tissue of irradiated Albino rats-Histopathological study. *Int J Theor Appl Sci* 2022; 1(1), 18-26.

54. Sorour HA, Salem MA, Abdelmaksoud DA, Elgalil A, Mohamed M. The Impact of High Fat Diet and Flaxseed on Liver Histology,

Histochemistry and Morphometry in Ovariectomized Albino Rat. *Egypt J Histol 2022;* 45(1), 68-89.

55. Zineldeen DH, Tahoon NM, Sarhan NI. AICAR Ameliorates Non-Alcoholic Fatty Liver Disease via Modulation of the HGF/NF-κB/SNARK Signaling Pathway and Restores Mitochondrial and Endoplasmic Reticular Impairments in High-Fat Diet-Fed Rats. *Int J Mol Sci 2023;* 24(4), 3367.

56. Ahishali E, Demir K, Ahishali B, Akyuz F, Pinarbasi B, Poturoglu S, et al. Electron microscopic findings in non-alcoholic fatty liver disease: Is there a difference between hepatosteatosis and steatohepatitis?. *J gastroenterol Hepatol* 2010; 25(3), 619-26.

57. El-Desoky F, Gaber AEH, Holah NS, Esam EL, Daba MHY, Abd Elrahman AY, et al. Protective effect of caffeine and curcumin versus Silymarin on nonalcoholic steatohepatitis in rats. *Menoufia Med J* 2020; 33(1), 196.

58. Guo Y, Wang S, Wang Y, Zhu T. Silymarin improved diet-induced liver damage and insulin resistance by decreasing inflammation in mice. *Pharm Biol* 2016; 54(12), 2995-3000.

59. Doostkam A, Fathalipour M, Anbardar MH, Purkhosrow A, Mirkhani H. Therapeutic Effects of Milk Thistle (Silybum marianum L.) and Artichoke (Cynara scolymus L.) on Nonalcoholic Fatty Liver Disease in Type 2 Diabetic Rats. *Can J Gastroenterol Hepatol* 2022; 2022:2868904.

60. Kalopitas G, Antza C, Doundoulakis I, Siargkas A, Kouroumalis E, Germanidis G, et al. Impact of Silymarin in individuals with nonalcoholic fatty liver disease: A systematic review and meta-analysis. *Nutrition* 2021; 83:111092.

61. Vargas-Mendoza N, Ángeles-Valencia M, Madrigal-Santillán EO, Morales-Martínez M, Tirado-Lule JM, Solano-Urrusquieta A, et al. A. Effect of Silymarin supplementation on physical performance, muscle and myocardium histological changes, bodyweight, and food consumption in rats subjected to regular exercise training. *Int J Mol Sci* 2020; 21(20): 7724.

62. Wang L, Zhang L, Gan K, Hua X, Xiao Y, Shi Y, Tan Z. Comparative effect on liver fibrosis of bicyclol and Silymarin. *Afr J Pharm Pharmacol* 2020; 14(4): 77-86.

63. Yassin N, AbouZid SF, El-Kalaawy AM, Ali TM, Elesawy BH, Ahmed OM. Tackling of renal carcinogenesis in wistar rats by Silybum marianum total extract, Silymarin, and silibinin via modulation of oxidative stress, apoptosis, Nrf2, PPARγ, NF-κB, and PI3K/Akt signaling pathways. *Oxid Med Cell Longev* 2021;2021: 7665169.

64. Zhang Z, Li X, Sang S, McClements DJ, Chen L, Long J, et al. A review of nanostructured delivery systems for the encapsulation, protection, and delivery of Silymarin: An emerging nutraceutical. *Food Res Int* 2022; 156: 111314.

65. Elshemy MM, Asem M, Allemailem KS, Uto K, Ebara M, Nabil A. Antioxidative capacity of liver-and adipose-derived mesenchymal stem cell-conditioned media and their applicability in treatment of type 2 diabetic rats. Oxidative medicine and cellular longevity. *Oxid Med Cell Longev* 2021; 2021: 8833467.

66. Tan HL, Guan XH, Hu M, Wu J, Li RZ, Wang LF, et al. Human amniotic mesenchymal stem cells-conditioned medium protects mice from high-fat diet-induced obesity. *Stem Cell Res Ther* 2021; 12(1), 1-14.

67. Ravan AP, Goudarzi F, Rafieemehr H, Bahmani M, Rad F, Jafari M, et al. Human umbilical cord-mesenchymal stem cells conditioned medium attenuates CCl4 induced chronic liver fibrosis. *Toxin rev* 2019; 40: 238-49

68. Ra K, Oh HJ, Kim GA, Kang SK, Ra JC, Lee BC. High Frequency of Intravenous Injection of Human Adipose Stem Cell Conditioned Medium Improved Embryo Development of Mice in Advanced Maternal Age through Antioxidant Effects. *Animals* 2020; 10(6): 978.

69. Jin QH, Kim HK, Na JY, Jin C, Seon JK. Anti-inflammatory effects of mesenchymal stem cell-conditioned media inhibited macrophages activation in vitro. *Sci Rep* 2022; 12(1), 4754.

70. Laksmitawati DR, Noor SU, Sumiyati Y, Hartanto A, Widowati W, Pratami DK. The effect of mesenchymal stem cell-conditioned medium gel on burn wound healing in rat. *Vet World* 2022; 15(4), 841.

71. Squecco R, Tani A, Chellini F, Garella R, Idrizaj E, Rosa I, et al. Bone marrow-mesenchymal stromal cell secretome as conditioned medium relieves experimental skeletal muscle damage induced by ex vivo eccentric contraction. *Int J Mol Sci* 2021; 22(7): 3645.

72. Du Z, Wei C, Cheng K, Han B, Yan J, Zhang M, et al. Mesenchymal stem cell–conditioned medium reduces liver injury and enhances regeneration in reduced-size rat liver

transplantation. *J Surg Res* 2013; 183(2): 907-15.

73. Borges LF, Manetti M. Telocytes and Stem Cells. In Resident Stem Cells and Regenerative Therapy. Academic Press. 2024; 305-37

74. Mikłosz A, Nikitiuk BE, Chabowski A. Using adipose-derived mesenchymal stem cells to fight the metabolic complications of obesity: Where do we stand?. *Obes Rev* 2022; 23(5): e13413.

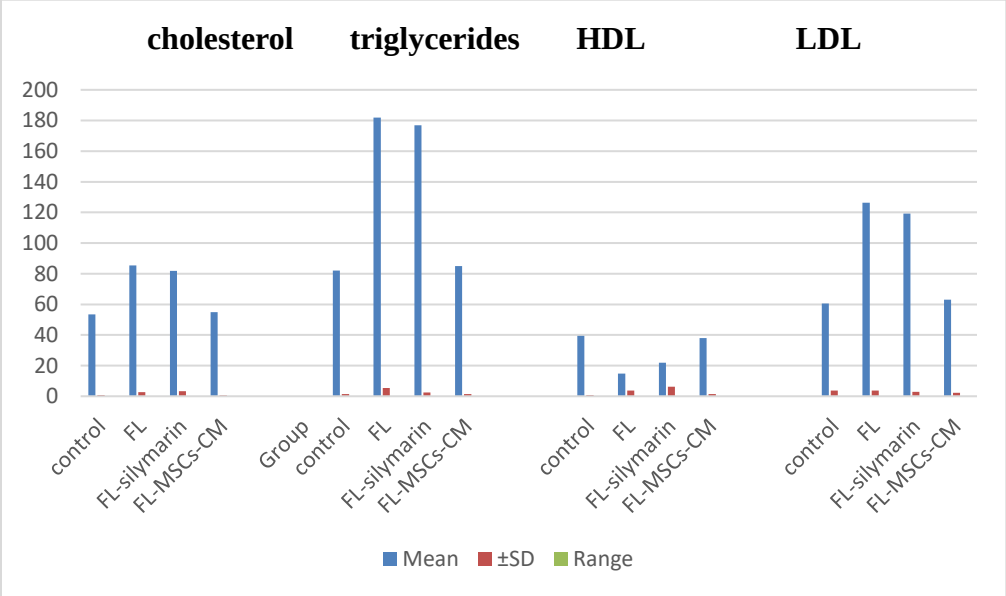

Figure (1s): Lipid profile expression in different studied groups.

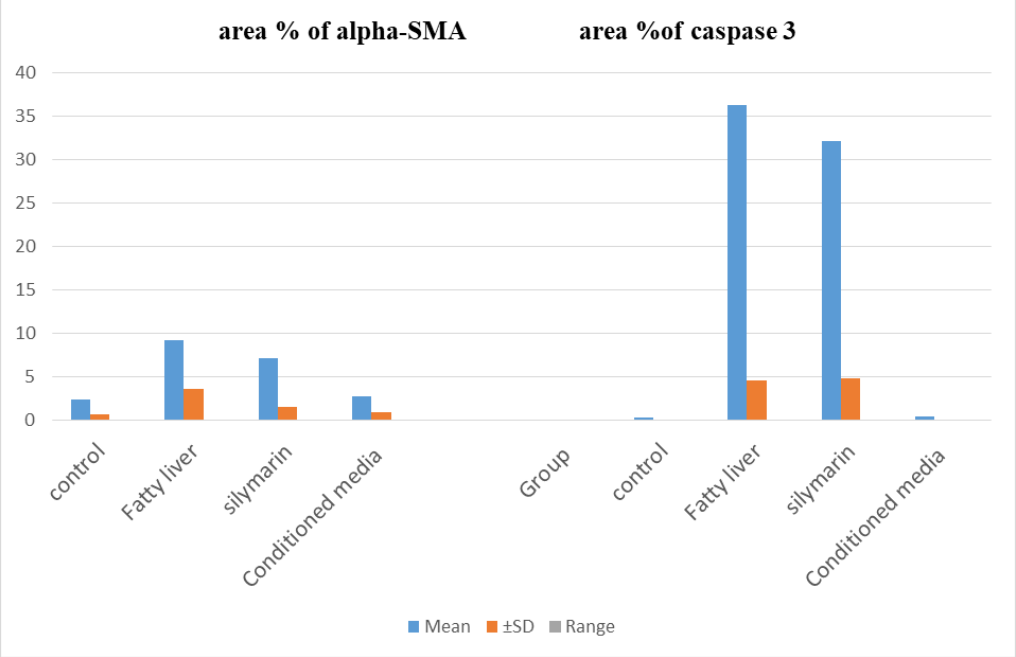

Figure (2s): Mean values of area percent of alpha smooth muscle actin and Caspase 3 immune reactions in different studied groups.

To Cite:

Hassan, E., Zidan, R., Mesiha, S., El-Mahroky, S. Effect of Mesenchymal Stem Cells-Conditioned Medium versus Silymarin on Experimentally Induced Fatty Liver in Adult Male Albino Rats (A Histological and Immunohistochemical Study). ***Zagazig University Medical Journal*****, 2024; (71-90): -. doi: 10.21608/zumj.2024.280708.3301**